HHS Public Access

Author manuscript

ACS Sens. Author manuscript; available in PMC 2019 January 26.

Published in final edited form as:

ACS Sens. 2018 January 26; 3(1): 143–150. doi:10.1021/acssensors.7b00764.

Visual Sensor for Sterilization of Polymer Fixtures Using Embedded Mesoporous Silicon Photonic Crystals

Tushar Kumeria[†,‡,#], **Joanna Wang**[§,#], **Nicole Chan**[†], **Todd J. Harris**[‖], and **Michael J Sailor**[*,†]

[†]Department of Chemistry and Biochemistry, University of California, San Diego, 9500 Gilman Drive, La Jolla, California 92093, United States

[§]Materials Science and Engineering Program, University of California, San Diego, 9500 Gilman Drive, La Jolla, California 92093, United States

[‡]School of Pharmacy, University of Queensland, 20 Cornwall Street, Woolloongabba, Queensland-4102, Australia

[‖]Sienna Biopharmaceuticals Inc., 30699 Russell Ranch Road, Suite 140, Westlake Village, California 91362, United States

Abstract

A porous photonic crystal is integrated with a plastic medical fixture (IV connector hub) to provide a visual colorimetric sensor to indicate the presence or absence of alcohol used to sterilize the fixture. The photonic crystal is prepared in porous silicon (pSi) by electrochemical anodization of single crystal silicon, and the porosity and the stop band of the material is engineered such that the integrated device visibly changes color (green to red or blue to green) when infiltrated with alcohol. Two types of self-reporting devices are prepared and their performance compared: the first type involves heat-assisted fusion of a freestanding pSi photonic crystal to the connector end of a preformed polycarbonate hub, forming a composite where the unfilled portion of the pSi film acts as the sensor; the second involves generation of an all-polymer replica of the pSi photonic crystal by complete thermal infiltration of the pSi film and subsequent chemical dissolution of the pSi portion. Both types of sensors visibly change color when wetted with alcohol, and the color reverts to the original upon evaporation of the liquid. The sensor performance is verified using *E. coli*-infected samples.

Graphical abstract

[*]**Corresponding Author:** msailor@ucsd.edu.

[#]**Author Contributions**

T. Kumeria and J. Wang contributed equally to this work

Supporting Information

The Supporting Information is available free of charge on the ACS Publications website at DOI: 10.1021/acssensors.7b00764.

SEM images; optical reflection spectra; water contact angle measurements; electron microscope images; porosity, thickness, and color of sensors values (table S1); bacterial counts on photonic sensors (table S2) PDF)

Videos of colorimetric sensing of alcohol with pSi-polymer composite, with all-polymer disks and with integrated IV connectors; Video showing leak test of sensor-embedded IV connector during buffer infusion (ZIP)

ORCID

Michael J Sailor: 0000-0002-4809-9826

Notes

The authors declare no competing financial interest.

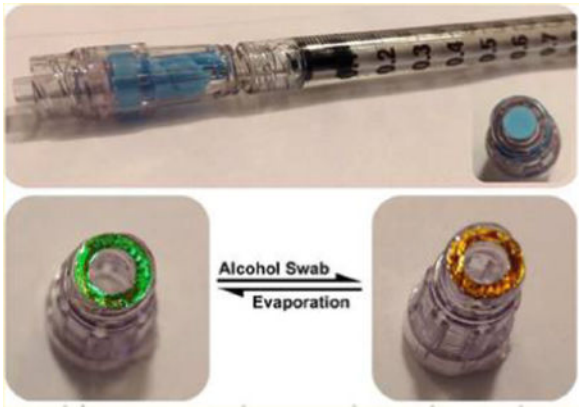

Keywords

needleless IV connectors; polycarbonate; phlebitis; E. coli bacteria; nanopores; mesoporosity; porous silicon

Intravascular (IV) catheters are among the most commonly used means of delivering therapeutics or for aspirating blood samples in hospitals and clinics worldwide. Despite widespread use, these devices are prone to bacterial colonization that puts patients at risk of local and systemic infections such as injection-site infection, catheter related-bloodstream infection, phlebitis, septic thrombophlebitis, endocarditis, and other complications. In the United States alone, more than 80,000 intravascular catheter-related complications are reported every year for patients in intensive care units, with an estimated 9600 to 20,000 deaths and an expense ranging from $296 million to $2.3 billion US annually.[1–4] Needle-less systems, where an IV line is placed in the patient and reused multiple times via a port or hub, are now common in healthcare settings, and they have led to substantial reductions in needle-stick injuries. Failure to properly disinfect the reusable injection port on such IV catheters is considered one of the more pervasive errors made by staff and health care professionals.[5] When not disinfected between administration sets, an IV connector hub can provide a source of infection, and when disinfected improperly, the infusion of residual disinfectants into the bloodstream can lead to phlebitis.[6–9] Phlebitis is an inflammation of the cannulated vein, and it is the most frequent complication associated with peripheral IV catheters, occurring in 27–70% of all the catheters deployed.[10–14] IV-related phlebitis is recognized as a problem by manufacturers, the Center for Disease Control (CDC), and the Infusion Nurses Society (INS).[15–22] This study was motivated by the desire to incorporate a sensor on an IV catheter connector hub that could provide a visual cue to the healthcare worker that the device has been disinfected, and furthermore indicate when the liquid sterilizing agent has been completely removed.

The approach used in this work is based on embedding a mesoporous photonic crystal into the surface of a plastic fixture.[23–25] Our group and others have shown that porous silicon (pSi) can be used as a template for solution-cast or heat-cast polymers,[26–31] and the resulting polymer-pSi composites or polymer replicas can retain the porous nanostructure of the template. By using a porous photonic crystal as the template, the polymer takes on the

spectral characteristics of the template, in particular, its ability to display a stop band in the reflectance spectrum, and the ability of this stop band to shift when infiltrated with a liquid —resulting in a color change that is readily observed with the unaided eye. For the present work, we employed thermal infiltration to either partially or completely infiltrate the template, and used an IV connector (BD-MaxPlus Clear) made of polycarbonate, which formed a viscous liquid that infiltrated the pores of the pSi host. Two types of sensors were prepared (Scheme 1): (a) a composite sensor, where the pSi template was fused to the polycarbonate surface, partially infiltrating the pSi film but leaving the majority of the pore structure open and available for sensing; and (b) an all-polymer sensor, where the pSi template was completely infiltrated with polymer and then removed by chemical dissolution. The sensor devices were tested for their ability to indicate the presence of disinfectant delivered by a commercial alcohol swab (70% isopropyl alcohol), and sterilization was confirmed using a nonpathogenic *E. coli* strain and a standard culturing assay.

RESULTS AND DISCUSSION

Fabrication of pSi Templates for the Photonic Sensors

The pSi templates for both types of sensors (polymer composite and all-polymer) were synthesized by electrochemical anodization of single-crystal silicon wafers in an aqueous ethanolic hydrofluoric acid electrolyte using a sinusoidal current–time profile as previously described.[23,32] Cross-sectional scanning electron microscope (SEM) images revealed the modulation in porosity as a series of light and dark bands spaced at approximately 150 nm and running parallel to the surface of the porous layer (Figure 1 and Figure S1, Supporting Information). The evenly spaced layers generate an optical rugate filter, displaying a stop-band in the reflection spectrum with a wavelength of maximum reflectance directly proportional to the spacing in the layers (Figure S2, Supporting Information).[33,34] Thus, the apparent color of the pSi template (and thus the resulting templated sensors) was readily engineered by adjusting the period of the sine wave that served as the current density–time waveform used in electrochemical anodization of the silicon wafer. Digital analysis of the plane-view SEM images (Figure S1a, Supporting Information) indicated a mean pore diameter of 19 ± 7 nm. Average porosity of the pSi template, measured by means of gravimetry and by the spectroscopic liquid infiltration method (SLIM),[23] was ~60% for both sensor types (Figure S2 and Table S1). For the pSi-polymer composite sensors, the pSi templates were designed to be thicker, containing more porous layers than the templates used for the all-polymer sensors. The thickness of the templates was measured by cross-sectional SEM, by SLIM, and by gravimetry, and they were on the order of ~60 μm thick for the pSi-polymer composite sensor templates and ~40 μm thick for the all-polymer sensor templates (Table S1).

Fabrication of pSi-Polymer Composite Photonic Sensors

One of the key motivations for constructing the composite sensors was to capitalize on the high refractive index contrast afforded by silicon. This can be expected to give a strong reflectance spectrum that is more readily seen by eye when the sensor is wetted with the disinfectant solution; for example, if the porous skeleton possesses a refractive index closely matching the value of the liquid disinfectant filling the pores, then the intensity of the stop

band reflectance will be near zero. The index of refraction of crystalline silicon in the wavelength range of interest is 3.8,[33] while the index of polycarbonate (1.58)[35] is closer to the index of 70% aqueous isopropanol (1.372 ± 0.001 at 22.6 °C, measured at λ = 589.3 nm) used as a disinfectant. Thus, we attempted to build a sensor element where only a small portion of the pSi film was infiltrated with polymer, in order to serve as an anchoring point, while the majority of the pSi layer remained open and exposed on the fixture surface to act as the sensor (Scheme 1).

The thermal infiltration process used to fabricate the pSi-polycarbonate composites was first optimized using hard polycarbonate disks, and a range of temperatures and infiltration times was explored. To improve polymer infiltration and avoid drift of the optical spectrum during processing, the pSi templates were partially oxidized by heating at 500 °C for 2 h in air prior to polymer infiltration. This treatment generated a thin oxide shell on the pSi skeleton. Filling of pores by polymers is a complex process that is highly dependent on the pore size of the host and the viscosity of the polymer.[26,36] In the present case, the optimal thermal infiltration procedure was determined to be as follows: the polycarbonate disk was placed on top of the pSi photonic crystal template, the assembly was heated at 185 °C for 2 h, and then the temperature was increased to 230 °C and the device was maintained at that temperature for an additional 12 h. We found that the first step of heating at 185 °C was effective in avoiding the formation of air bubbles in the polymer. The second heating step yielded relatively complete infiltration of the pores. Upon cooling, the polymer-infiltrated pSi layer spontaneously detached from the underlying bulk silicon wafer due to stresses associated with solidification of the polymer and differences in the thermal expansion coefficients of silicon and polycarbonate, resulting in a freestanding pSi-polymer composite. The open pore structure of the pSi template was readily observed on the detached side of the film (Figure 1a), indicating that the polymer did not fully infiltrate the nanostructure. This was confirmed by optical reflectance measurements (Figure S3, Supporting Information) and with cross-sectional SEM measurements (Figure 1b). Energy dispersive X-ray spectroscopy (EDS) was employed in the SEM to confirm the infiltration of polymer into the pSi template, and it indicated that the polymer penetrated to depths of between 7 and 10 μm into the 60-μm-thick pSi templates (Figure 1b,e). This is consistent with the optical measurements; the reflection spectrum from the composite film displayed two distinct stop bands, one at the wavelength corresponding to the air-filled pSi template (λ_{sb} = 520 nm) and another, weaker band (λ_{sb} = 660 nm) arising from the polycarbonate-filled region of the pSi template (Figure S3, Supporting Information). The imprinting process (i.e., infiltration of polymer into the pSi master to replicate its nanostructure) yielded comparable morphological and spectral characteristics when commercial polycarbonate IV connector hubs were used in place of the polycarbonate disks (Figure 2).

Fabrication of All-Polymer Photonic Sensors

Whereas the pSi-polymer composite sensors displayed strong, readily observable colors due to the high refractive index of the silicon skeleton, the presence of silicon, or any material other than the medical-grade polycarbonate of the fixture raises concerns about potential contamination or adverse reactions of fluids contacting the device. Therefore, we also explored an alternative device design where the photonic sensor was composed completely

of polycarbonate. This approach relied on the ability of the pSi material to serve as a removable template for polymer casting that can be selectively removed by a chemical etchant.[27] There are a few chemical systems that can selectively remove silicon: the well-known xenon difluoride etchant used in the manufacture of silicon MEMS,[37] strongly alkaline solutions such as aqueous KOH,[23] and mixtures of dimethyl sulfoxide and aqueous HF.[38] In this work we chose to use the dimethyl sulfoxide/aqueous HF etchant due to its low reactivity with polycarbonate.

The dimethyl sulfoxide (DMSO) in the dimethyl sulfoxide/aqueous HF system acts as a mild chemical oxidant, converting silicon to silicon dioxide. In the presence of aqueous HF, the oxide product then dissolves. The relatively low surface tension of DMSO allows the etchant solution to penetrate the mesoporous structure, allowing efficient removal of the pSi skeleton.[38,39] In the present case, the procedure was sufficiently mild that the polymer retained a replica of the nanostructure of the original pSi template (Figure 1f), and the resulting all-polymer nanostructure displayed the optical properties of a photonic crystal (Figure S3, Supporting Information). However, because the wavelength of the stop band depends on the volume fraction and the index of refraction of the skeleton, the stop band of the resulting polycarbonate replicas was substantially blue-shifted from the stop band of the original pSi templates. Thus, the stop band of the pSi template used for the all-polymer photonic sensors was engineered with a periodicity appropriate to yield the desired color in the final system (Table S1, Supporting Information). The imprinting process yielded similar results with commercial polycarbonate IV connector hubs as it did with polycarbonate disks (Figure 2).

Sensing of Alcohol Sterilization Solutions Using the Photonic Devices

The ability of the pSi-polymer composite and the all-polymer photonic devices to detect the presence of 70% isopropyl alcohol disinfecting solutions was then assessed by optical reflectance spectroscopy and by visual inspection. A distinctive red shift in the stop-band of >60 nm was observed for either the pSi-polymer or the all-polymer photonic sensor disks. The visual appearance of the pSi-polymer composite changed from green to red upon addition of the alcohol disinfectant (Figure 2a and Figure S3a), and for the all-polymer photonic structure the color changed from blue to light green (Figure 2b and Figure S3b). The spectral observations for the imprinted commercial polycarbonate IV connector hubs were similar to those of the polycarbonate disk test articles, although the net spectral shifts upon alcohol infiltration were somewhat smaller for the IV connector hub devices (65 nm vs 80 nm for the composite sensors and 40 vs 60 nm for the all-polymer sensors). This implies that the porosity of the photonic crystal was somewhat lower for the IV connector hubs relative to the polycarbonate disk test articles, and suggests that the polycarbonate comprising the IV connector hubs did not infiltrate the pSi templates as fully as the polycarbonate comprising the test disks. The difference in flow behavior is not surprising, as the hubs and the disks derived from different manufacturers, and it is unlikely that the viscosity, molecular weight, and other fundamental properties of the two types of polycarbonate test articles used in this study were the same. Although we confirmed that both comprised polycarbonate by FTIR measurements, we did not measure viscosity, average molecular weight, or other properties of the polymer samples.

The photonic stop-band for both the photonic sensors returned to their original values after evaporation of the disinfectant (Videos S1–S4, Supporting Information). Both types of devices were able to visually report complete evaporation of the disinfectant, although the intensity of the stop band displayed by the all-polymer devices was distinctively weaker and more difficult to discern than for the pSi-polymer composites. The weaker reflection from the all-polymer rugate filters is consistent with the lower refractive index contrast between polycarbonate and the medium filling the pores (either air or alcohol) relative to the index contrast between silicon and these same media, as discussed above and elsewhere.[24,34,40] The color changes were stable and reproducible over repeated wetting and air-drying cycles (Figure 2c,d). Direct addition of 70% isopropyl alcohol (20 μL) into these devices required 2–3 min to completely evaporate and for the original color to return.

A concern with colorimetric sensors is that a fraction of the human population is color-blind and so may not readily be able to distinguish blue-to-green or green-to-red color changes. For this reason we explored the possibility of tuning the spectral band of the photonic sensor to the red, such that liquid infiltration shifted the stop band into the near-infrared region of the spectrum (Figure S4, Supporting Information). The visual perception to a completely color-blind person (or in a grayscale image) in this case was a distinctive change from light to dark upon liquid infiltration.

Sensor Performance under a Bacterial Challenge

In order to validate the sensors in a realistic complex matrix, we exposed the photonic sensors embedded in IV connectors to growth media containing bacteria. There were two main goals of these experiments: first, we wanted to evaluate if contaminants would collect in the nanoporous matrix of the sensors, fouling the optical response. Second, it is known that bacteria can accumulate on porous media, and there is a potential that such surfaces may enhance bacterial colonization and growth and thus be more difficult to sterilize.[41–44] The sensors were incubated in 2×10^6 CFU/mL of nonpathogenic *E. coli* (FDA strain Seattle 1946) in Luria–Bertani (LB) media for 4 h. Subsequently, the sensors were thoroughly rinsed with DI water and then scraped with an inoculation loop to collect the adhered bacteria, which were then cultured on agar plates to determine the number of colony-forming units (CFUs). We detected $(1.5 \pm 0.4) \times 10^5$ CFU/mL on the pSi-polymer composite photonic sensors and $(7 \pm 2) \times 10^4$ CFU/mL on the all-polymer photonic sensors (Table S2, Supporting Information). The observed difference in the number of CFUs found on the two types of sensors can be attributed to differences in their wettability, which is known to influence bacterial adhesion.[45] Water contact angle (WCA) measurements (Figure S5, Supporting Information) showed that the pSi-polymer composite photonic sensors, which displayed the higher degree of bacterial attachment, were also substantially more hydrophilic (WCA = 11.6°) compared to the relatively hydrophobic all-polymer photonic sensors (WCA = 113.8°).

Another set of sensors were subjected to the same *E. coli* incubation procedure and then swabbed with alcohol wipes following the sterilization procedure recommended by the U.S. Center for Disease Control (30 s to 2 min, wipe saturated with 70% isopropyl alcohol).[16] After the sterilization procedure, the surface of the samples was assayed for the presence of

live bacteria as described above. No live *E. coli* were observed to survive this procedure (to a detection limit of 25 CFU/mL). We also analyzed the porous sensor surfaces by electron microscopy to determine the fate of adhered *E. coli* post-sterilization. Electron microscope images of the surface of the sensor devices after contact with the alcohol swab showed evidence of ruptured *E. coli* cells; consistent with the lack of CFUs observed after sterilization (Figure S6, Supporting Information).

The optical changes exhibited by the sensors during the infection and sterilization processes were monitored using reflection spectroscopy and visual assessment. The pSi-polymer composite photonic sensors, being more hydrophilic,[26] were infiltrated by aqueous solutions and thus exposure to the culture media induced a color change (red shift) similar to that observed upon alcohol sterilization. When the samples dried the color blue-shifted back to the original, air-filled values. Subsequent sterilization with alcohol generated the expected red shifts in color, analogous to what was observed with the pristine sensors. Thus, the color changes observed with the pSi-polymer composite photonic sensors could not clearly distinguish between the alcohol sterilization solution and a bacteria-infected liquid medium. By contrast, the all-polymer photonic sensors were more hydrophobic (Figure S5, Supporting Information); the aqueous culture media did not readily infiltrate the nanopores, and no substantial change in color was observed when this sensor type was incubated with the bacteria culture medium. As with the pSi-polymer composite photonic sensors, the expected color changes were observed upon subsequent sterilization with alcohol. Thus, the all-polymer system is more reliable from the perspective of the colorimetric assay: due to the hydrophobic nature of the sensor, the green-to-red color change was only observed with alcohol solutions and not with water-based solutions.

The nanoporous nature of the sensor elements could be a potential source of leaks in a connector hub. We tested the integrated IV connector hub-sensor units for leakage under simulated infusion conditions, and observed no visible fluid leakage after 10 usage cycles (Video S5, Supporting Information). We also evaluated whether or not silicon (in the form of water-soluble orthosilicate) would leach into the infusate from the pSi-polymer composite photonic devices. The silicon content in the infusate (PBS) was measured using the molybdenum blue assay,[46] which showed no detectable (LOD = 0.5 ppm) silicon in 1 mL of infusate after 30 min of contact with the sensor hub. For comparison, the concentration of silicon in human plasma is 5 ppm.[47–49]

It should be noted that the sensor described in this work is designed to function in a specific clinical environment, and a main limitation of the sensor is that it is nonspecific, responding with a color change to essentially any liquid that infiltrates the mesoporous structure. Thus, contamination of the sensor surface with IV fluids that can infiltrate but that are not readily removed from the nanoporous matrix is a concern. It is worth noting that modern IV connectors are designed to minimize the possibility of IV fluid leakage; the BD-MaxPlus Clear IV needleless connector used in this study is an anti-reflux connector that is specifically designed to minimize the possibility of leakage of IV fluid into the region where the sensor surface is located during priming, flushing, and aspiration.

Another concern related to integrating these visual sensors with an IV connector is the mechanical stability of the sensor. Although we did not perform extensive mechanical tests, we did not observe any signs of mechanical wear or degradation during repeated swabbing with alcohol (Videos S3 and S4, Supporting Information) or during repeated infusion of buffer solutions through the sensor-integrated IV device (Video S5, Supporting Information). These latter experiments involved connecting and disconnecting a luer lock syringe to the IV connector for each flushing procedure.

In summary, this study explored the potential for embedding pSi photonic sensors into reusable medical devices as a visual aid to effective sterilization. We employed needleless IV connector hubs as test fixtures, and evaluated two types of sensors consisting of polycarbonate thermally cast into pSi photonic crystal templates: a composite consisting of pSi and polycarbonate, and an all-polycarbonate device from which the pSi template had been selectively removed. Both types of sensors displayed distinctive color changes that reported on the infiltration and the evaporation of a 70% isopropyl alcohol disinfectant. The pSi-polymer composite sensor displayed more intense colors and color changes that were more visually distinct, but the all-polymer sensor was more effective at repelling water-based solutions that could potentially act as false positives for the presence of the alcohol sterilizing agent. The sensor-embedded IV connector units could be used multiple times without any degradation in optical response, leakage, or leaching of silicon into a test infusate.

EXPERIMENTAL SECTION

Materials

Single-crystal silicon wafers, highly boron-doped (p-type), of resistivity 1 mΩ·cm, and thickness 525 ± 25 μm and polished on the (100) face were purchased from Virginia Semiconductor. Absolute ethanol (200 proof) was obtained from VWR International Corp. Hydrofluoric acid (48% aqueous, ACS grade) was obtained from Macron Chemicals. Potassium hydroxide (ACS grade, 85%) was purchased from Fisher Scientific Chemicals, Inc. Phosphate buffered saline (PBS) solution and Hank's buffered saline solution (HBSS) was purchased from Gibco, Inc. Aqueous solutions were prepared from 18 MΩ deionized water (DI). Clear polycarbonate sheets were purchased from eplastic, inc. (HYGARD MS1250 CLEAR-A00, 040 in. thick). BD MaxPlus Clear IV connectors were purchased from the manufacturer. Identity of the polymers was confirmed by FTIR (strong bands at 1769, 1503, 1219, 1187, and 1158 cm^{-1} characteristic of polycarbonate).

Preparation of pSi Photonic Crystal Templates

Different pSi rugate filter templates were used for the pSi-polymer composite and the all-polymer sensors. Both types of pSi photonic crystals were etched into the highly doped silicon samples by electrochemical anodization (Keithley Sourcemeter model 2651, Tektronix, USA) in aqueous ethanolic hydrofluoric acid (3:1 *v*:*v* 48% aqueous HF:ethanol) electrolytes following published procedures.[23] *Caution: HF is highly toxic and contact with skin should be avoided.* Anodization of the wafers was preceded by a "sacrificial etch" step to prepare clean and reproducible silicon surfaces. The sacrificial etch was carried out at

constant current density (100 mA cm^{-2}) for 30 s, which generated a thin porous silicon layer. This layer was then completely removed by immersion in a 2 M aqueous solution of potassium hydroxide (KOH). The pSi photonic crystal templates for the pSi-polymer compsite sensor were prepared by application of a sinusoidal current density-time profile (minimum current density: 100 mA cm^{-2}, maximum current density: 200 mA cm^{-2}, period: 2.6 s, 300 cycles). The templates were then thermally oxidized in a muffle furnace (Thermolyne, Thermo Fisher, USA) at 500 °C for 4 h (including the time for temperature ramp of 10 °C/min from/to ambient for both the heating and cooling phases). For the pSi photonic crystal templates used to prepare the all-polymer sensors, the current density limits and the period of the waveform were the same as for the pSi-polymer composite devices, but the number of cycles was 250, resulting in a thinner pSi template. The thermal oxidation (500 °C) was carried out for 2 h.

Polymer Infiltration into pSi Photonic Crystal Templates

All polymers were thermally infiltrated into the pSi templates by placing the polymer onto the template and heating it above the glass transition temperature of the polymer (210 °C). To prepare the pSi-polymer composite and the all-polymer photonic disks, a polycarbonate sheet (~1.5 cm × 1 cm) was placed on top of the pSi template and preheated to 185 °C on a hotplate (in air). After 2 h at 185 °C, the temperature was raised to 210 °C and infiltration was allowed to proceed for 16–18 h. The samples were allowed to cool to room temperature, and they were then immersed in liquid nitrogen. The rapid cooling usually resulted in fracture at the polymer/silicon substrate interface, generating freestanding pSi-polymer composites. The resulting pSi-composite sensors were then cut into disks with a diameter of 5 mm using a metal hole punch and used as-is. The all-polymer sensor disks were prepared from these pSi-composites by soaking in a solution consisting of 1 part dimethyl sulfoxide (DMSO), 3 parts 48% aqueous HF, and 1 part ethanol for 18 h. This solution has been shown to effectively remove Si and SiO_2 from composite pSi structures.[39] Polymer infiltration of IV connector hub units (BD-MaxPlus Clear) was carried out using the above thermal infiltration process, where the IV connectors were placed onto the pSi substrate and heated to 185 °C for 2 h. The connectors were pressed to the surface to ensure contact of the sensor to the silicon. The temperature was then increased to 210 °C for 10–18 h. To prepare the all-polymer IV connector hub sensors, the pSi template was removed by soaking in DMSO/HF/EtOH (1:3:1) for 8 h.

Scanning Electron Microscopy and EDS Analysis

Samples were imaged using a Zeiss Sigma 500 scanning electron microscope (SEM) with at an accelerating voltage of 1 kV. The samples were coated with iridium using a sputter coater prior to imaging to prevent charging. The energy dispersive X-ray spectra (EDS) were obtained using a Philips XL30 field emisson SEM fitted with an EDS detector (iXRF Systems, inc), operating at an acellerating voltage of 20 kV and using integration times of 50 s. Images were processed and analyzed using ImageJ software (public domain program, NIH). SEM images of bacteria were obtained ater sequential dehydration in decreasing concentrations of ethanol (100% *v*/*v* to 0% *v*/*v*).

Optical Characterization

Reflectance spectra were acquired using a CCD spectrometer (Ocean Optics USB-4000) fitted to a bifurcated fiber optic cable as previously described.[23] One arm of the optical fiber was connected to the spectrometer, while the other arm was connected to a tungsten light source (Ocean Optics LS-1). The distal end of the combined fiber was attached to a focusing lens to allow acquisition of 180° reflectance spectra from the sample surface, with a spot size of approximately 2 mm in diameter. The porosity and thickness of the samples was calculated using the spectroscopic liquid infiltration method (SLIM) described previously.[23,50] For the measurements involving repeated wetting/drying cycles, the sensor sample was firmly clamped to an optical table and the spectrometer was configured to acquire a spectrum every minute for a period of 2 h. A baseline signal was acquired for 10 min and then an aliquot (10 μL) of 70% isopropyl alcohol was applied to the surface of the sensor. After approximately 3 min the sample was dried in a stream of compressed air. The sample was then allowed to sit in air for an additional 3 min and the next aliquot of alcohol was applied, up to a total of 10 applications. Refractive index of liquids was measured with a Refracto 30GS (Mettler Toledo). Digital photographs were obtained using a Canon Rebel XT1 digital camera fitted with a macro lens.

Bacteria Culture and Sterilization Procedures

A nonpathogenic *E. coli* strain, FDA strain Seattle 1946, was obtained from American Type Culture Collection (ATCC). A single colony of *E. coli* was inoculated into Luria–Bertani (LB) media (COR Biosciences, USA) and incubated overnight at 37 °C. The culture was then washed three times with PBS (pH 7.4) by centrifugation (Centrifuge 5804, Eppendorf, 4200×*g*, 5 min) and resuspended in 10 mL of buffer. The culture was diluted to an optical density (OD) of 0.1 (measured at 600 nm), corresponding to 10^8 CFU/mL.[51,52] In order to assess the efficiency of sterilization of infected sensors, the culture was diluted to 2×10^6 CFU/mL and the devices were incubated in the mixture for 4 h. The samples were then rinsed briefly with water and scrubbed with a 70% isopropyl alcohol saturated swab (Webcol alcohol pads, Covidien) for 30–60 s, following the published protocol.[22] In order to assay for remaining live bacteria, the sample surface was thoroughly scraped with a heat sterilized inoculation loop and the bacteria collected in 200 μL of sterile water. For each sample, four dilutions of bacteria were prepared 0×, 100×, 1000×, and 10000× in sterile water and streaked onto an agar plate (Prepoured Agar BioRad). The plate was incubated at 37 °C for 16 h and the number of CFUs was determined by counting the colonies and accounting for appropriate dilution. Only the agar plates that contained 25–250 colonies per plate were considered in the CFU/mL calculation.

Si Leaching Tests

The IV connector-sensor device was attached to a 1 mL syringe filled with 1 mL HBSS that was pushed through the IV connector into a glass vial. The delivered volume was measured taking into account the dead volume in the syringe and IV connector hub to test for gross leakage. The delivered solution was tested for traces of dissolved silicon using the molybdenum blue (MB) assay. The MB assay reagents were prepared following the literature protocol:[46] Solution A was prepared by adding ammonium molybdate tetrahydrate

(1 g) and concentrated hydrochloric acid (3 mL) to 25 mL DI water, mixing, and then diluting in a volumetric flask with additional DI water to a total volume of 50 mL. For solution B, oxalic acid (4 g), 4-(methylamino)phenol hemisulfate (1.33 g), and anhydrous sodium sulfite (0.8 g) were added to 100 mL of DI water and mixed well. The solution was diluted in a volumetric flask with additional DI water to a total volume of 200 mL. For assaying, the test solution, solution A, and solution B were mixed in a volume ratio of 4:1:5 in an Eppendorf tube and incubated at room temperature for 1 h. The silicon content was quantified by measuring the absorbance at 810 nm and comparing to a standardized curve prepared from ICP standard of Si (TraceCERT, 1000 mg/L Si in nitric acid, Sigma-Aldrich).

Supplementary Material

Refer to Web version on PubMed Central for supplementary material.

Acknowledgments

This material is based upon work supported by the National Science Foundation under Grant No. CBET-1603177. JW thanks the NIH for a predoctoral training grant 2T32CA15391-06A1 (CRIN). The authors thank Tiffany K. Chen for experimental assistance.

References

1. O'Grady, NP., Alexander, M., Dellinger, EP., Gerberding, JL., Heard, S., Maki, D., Masur, H., McCormick, R., Mermel, L., Pearson, M. Draft guideline for the prevention of intravascular catheter-related infections. Centers for Disease Control; Atlanta, GA: 2001.
2. Pronovost P, Needham D, Berenholtz S, Sinopoli D, Chu H, Cosgrove S, Sexton B, Hyzy R, Welsh R, Roth G, Bander J, Kepros J, Goeschel C. An Intervention to Decrease Catheter-Related Bloodstream Infections in the ICU. N Engl J Med. 2006; 355:2725–2732. [PubMed: 17192537]
3. Zakhour R, Chaftari A-M, Raad II. Catheter-related infections in patients with haematological malignancies: novel preventive and therapeutic strategies. Lancet Infect Dis. 2016; 16:e241–e250. [PubMed: 27788992]
4. Wenzel RP, Edmond MB. Team-Based Prevention of Catheter-Related Infections. N Engl J Med. 2006; 355:2781–2783. [PubMed: 17192545]
5. Grissinger M. Capping Intravenous Tubing and Disinfecting Intravenous Ports Reduce Risks of Infection. P&T. 2011; 36:62–76. [PubMed: 21559311]
6. Schilling S, Doellman D, Hutchinson N, Jacobs BR. The impact of needleless connector device design on central venous catheter occlusion in children: a prospective, controlled trial. JPEN, J Parenter Enteral Nutr. 2006; 30:85–90. [PubMed: 16517952]
7. Niël-Weise BS, Stijnen T, van den Broek PJ. Should in-line filters be used in peripheral intravenous catheters to prevent infusion-related phlebitis? A systematic review of randomized controlled trials. Anesth Analg. 2010; 110:1624–1629. [PubMed: 20435946]
8. Chernecky C, Waller J. Comparative evaluation of five needleless intravenous connectors. J Adv Nurs. 2011; 67:1601–1613. [PubMed: 21366670]
9. Menyhay SZ, Maki DG. Preventing central venous catheter-associated bloodstream infections: Development of an antiseptic barrier cap for needleless connectors. Am J Infect Control. 2008; 36:S174.e1–S174.e5. [PubMed: 19084153]
10. Karadeniz G, Kutlu N, Tatlisumak E, Özbakkaloğlu B. Nurses' knowledge regarding patients with intravenous catheters and phlebitis interventions. J Vasc Nurs. 2003; 21:44–47. [PubMed: 12813411]
11. Perucca R, Micek J. Treatment of Infusion-Related Phlebitis Review and Nursing Protocol. J Infus Nurs. 1993; 16:282–286.

12. Maki DG, Ringer M. Risk factors for infusion-related phlebitis with small peripheral venous catheters: a randomized controlled trial. Ann Intern Med. 1991; 114:845–854. [PubMed: 2014945]
13. Grüne F, Schrappe M, Basten J, Wenchel H, Tual E, Stützer H. Phlebitis rate and time kinetics of short peripheral intravenous catheters. Infection. 2004; 32:30–32. [PubMed: 15007740]
14. Macklin D. Phlebitis: A painful complication of peripheral IV catheterization that may be prevented. Am J Nurs. 2003; 103:55–60. [PubMed: 12582339]
15. Frank MJ, Schaffner W. Contaminated aqueous benzalkonium chloride - unnecessary hospital infection hazard. J Am Med Assoc. 1976; 236:2418–2419.
16. O'Grady NP, Alexander M, Burns LA, Dellinger EP, Garland J, Heard SO, Lipsett PA, Masur H, Mermel LA, Pearson ML, Raad II, Randolph AG, Rupp ME, Saint S. Guidelines for the Prevention of Intravascular Catheter-related Infections. Clin Infect Dis. 2011; 52:e162–e193. [PubMed: 21460264]
17. Curran ET, Coia JE, Gilmour H, McNamee S, Hood J. Multi-centre research surveillance project to reduce infections/phlebitis associated with peripheral vascular catheters. J Hosp Infect. 2000; 46:194–202. [PubMed: 11073728]
18. Wide BW. MaxPlus clear needleless connector in-service video. MaxPlus clear needleless connector. 2016
19. Moureau NL, Flynn J. Disinfection of needleless connector hubs: clinical evidence systematic review. Nurs Res Pract. 2015; 2015:1.
20. Moureau NL, Dawson RB. Keeping needleless connectors clean, part 1. Nursing2010. 2010; 40:18–19.
21. Moureau NL, Dawson RB. Keeping needleless connectors clean, part 2. Nursing2010. 2010; 40:61–63.
22. Kaler W, Chinn R. Successful disinfection of needleless access ports: a matter of time and friction. J Vasc Access. 2007; 12:140–142.
23. Sailor, MJ. Porous Silicon in Practice: Preparation, Characterization, and Applications. Wiley-VCH; Weinheim, Germany: 2012. p. 57
24. Lorenzo E, Oton CJ, Capuj NE, Ghulinyan M, Navarro-Urrios D, Gaburro Z, Pavesi L. Porous silicon-based rugate filters. Appl Opt. 2005; 44:5415–5421. [PubMed: 16161654]
25. Salem MS, Sailor MJ, Sakka T, Ogata YH. Electrochemical preparation of a rugate filter in silicon and its deviation from the ideal structure. J ApplPhys. 2007; 101:063503.
26. Wang J, Lee GY, Kennard R, Barillaro G, Bisiewicz RH, Cortez Lemus NA, Cao XC, Anglin EJ, Park JS, Potocny A, Bernhard D, Li J, Sailor MJ. Engineering the Properties of Polymer Photonic Crystals with Mesoporous Silicon Templates. Chem Mater. 2017; 29:1263–1272.
27. Li YY, Cunin F, Link JR, Gao T, Betts RE, Reiver SH, Chin V, Bhatia SN, Sailor MJ. Polymer Replicas of Photonic Porous Silicon For Sensing and Drug Delivery Applications. Science. 2003; 299:2045–2047. [PubMed: 12663921]
28. Li YY, Kollengode VS, Sailor MJ. Porous silicon/polymer nanocomposite photonic crystals by microdroplet patterning. Adv Mater. 2005; 17:1249–1251.
29. Irani YD, Tian Y, Wang MJ, Klebe S, McInnes SJ, Voelcker NH, Coffer JL, Williams KA. A novel pressed porous silicon-polycaprolactone composite as a dual-purpose implant for the delivery of cells and drugs to the eye. Exp Eye Res. 2015; 139:123–131. [PubMed: 26277579]
30. Coffer, JL. Porous silicon and related composites as functional tissue engineering scaffolds. In: Santos, HA., editor. Porous Silicon for Biomedical Applications. 2014. p. 470-485.
31. Bonanno LM, Segal E. Nanostructured porous silicon-polymer-based hybrids: from biosensing to drug delivery. Nanomedicine. 2011; 6:1755–1770. [PubMed: 22122584]
32. Wang J, Joo J, Kennard RM, Lee S-W, Sailor MJ. Thermolytic Grafting of Polystyrene to Porous Silicon. Chem Mater. 2016; 28:79–89.
33. Berger MG, Arens-Fischer R, Thoenissen M, Krueger M, Billat S, Lueth H, Hilbrich S, Theiss W, Grosse P. Dielectric filters made of porous silicon: advanced performance by oxidation and new layer structures. Thin Solid Films. 1997; 297:237–240.
34. Bovard BG. Rugate filter theory: an overview. Appl Opt. 1993; 32:5427–5442. [PubMed: 20856352]

35. Kieser B, Dieterle F, Gauglitz G. Discrimination of methanol and ethanol vapors by the use of a single optical sensor with a microporous sensitive layer. Anal Chem. 2002; 74:4781–4787. [PubMed: 12349983]
36. Shin K, Obukhov S, Chen J-T, Huh J, Hwang Y, Mok S, Dobriyal P, Thiyagarajan P, Russell TP. Enhanced mobility of confined polymers. Nat Mater. 2007; 6:961–965. [PubMed: 17934464]
37. Pister, KSJ. Etchants for use in micromachining of CMOS Microaccelerometers and microelectromechanical devices and method of making the same. U S Patent No 5,726,480. 1998.
38. Anglin EJ, Schwartz MP, Ng VP, Perelman LA, Sailor MJ. Engineering the chemistry and nanostructure of porous silicon Fabry-Pérot films for loading and release of a steroid. Langmuir. 2004; 20:11264–11269. [PubMed: 15568884]
39. Kelly TL, Gao T, Sailor MJ. Carbon and Carbon/Silicon Composites Templated in Microporous Silicon Rugate Filters for the Adsorption and Detection of Organic Vapors. Adv Mater. 2011; 23:1776–1781. [PubMed: 21374740]
40. Pervak V, Tikhonravov AV, Trubetskov MK, Pistner J, Krausz F, Apolonski A. Band filters: two-material technology versus rugate. Appl Opt. 2007; 46:1190–1193. [PubMed: 17318237]
41. Massad-Ivanir, N., Segal, E. Porous silicon for bacteria detection. In: Santos, HA., editor. Porous Silicon for Biomedical Applications. 2014. p. 286-303.
42. Mirsky Y, Nahor A, Edrei E, Massad-Ivanir N, Bonanno LM, Segal E, Sa'ar A. Optical biosensing of bacteria and cells using porous silicon based, photonic lamellar gratings. Appl Phys Lett. 2013; 103:033702.
43. Wu C-C, Alvarez SD, Rang CU, Chao L, Sailor MJ. Label-free Optical Detection of Bacteria on a 1-D Photonic Crystal of Porous Silicon. Proc SPIE. 2010; 7167:71670Z–10.
44. Letant SE, Hart BR, Van Buuren AW, Terminello LJ. Functionalized silicon membranes for selective bio-organism capture. Nat Mater. 2003; 2:391–396. [PubMed: 12717430]
45. Lorenzetti M, Dogša I, Stošicki T, Stopar D, Kalin M, Kobe S, Novak S. The Influence of Surface Modification on Bacterial Adhesion to Titanium-Based Substrates. ACS Appl Mater Interfaces. 2015; 7:1644–1651. [PubMed: 25543452]
46. Low SP, Voelcker NH, Canham LT, Williams KA. The biocompatibility of porous silicon in tissues of the eye. Biomaterials. 2009; 30:2873–2880. [PubMed: 19251317]
47. Jugdaohsingh R. Silicon and bone health. J Nutr Health Aging. 2007; 11:99–110. [PubMed: 17435952]
48. Canham LT. Nanoscale semiconducting silicon as a nutritional food additive. Nanotechnology. 2007; 18:185704.
49. Anderson SHC, Elliott H, Wallis DJ, Canham LT, Powell JJ. Dissolution of different forms of partially porous silicon wafers under simulated physiological conditions. Phys Status Solidi A-Appl Res. 2003; 197:331–335.
50. Segal E, Perelman LA, Cunin F, DiRenzo F, Devoisselle J-M, Li YY, Sailor MJ. Confinement of Thermoresponsive Hydrogels in Nanostructured Porous Silicon Dioxide Templates. Adv Funct Mater. 2007; 17:1153–1162.
51. Pal S, Tak YK, Song JM. Does the antibacterial activity of silver nanoparticles depend on the shape of the nanoparticle? A study of the gram-negative bacterium Escherichia coli. Appl Environ Microbiol. 2007; 73:1712–1720. [PubMed: 17261510]
52. Cai Z, Kwak DH, Punihaole D, Hong Z, Velankar SS, Liu X, Asher SA. A photonic crystal protein hydrogel sensor for Candida albicans. Angew Chem, Int Ed. 2015; 54:13036–13040.

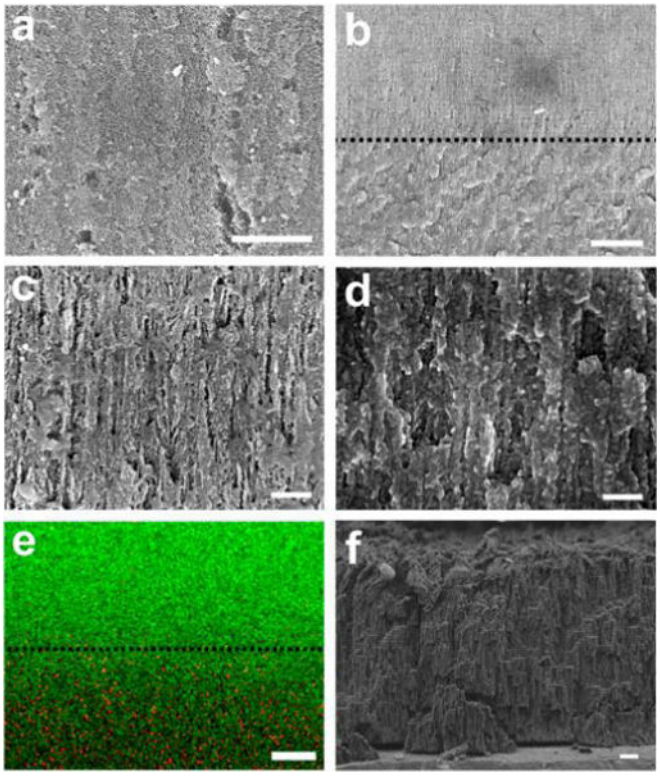

Figure 1.

SEM images of pSi-polymer composite photonic sensor element consisting of a pSi template partially infiltrated with polycarbonate. (a) Plan view of the pSi template on the side opposite the polymer layer, showing the open pore structure of the template with no detectable polymer. Scale bar: 1 μm. (b) Cross-sectional image showing the interface between the polymer-infiltrated region of the pSi film and the empty region of the pSi film. The layered nanostructure corresponding to the periodic porosity gradient that was generated during electrochemical preparation of the pSi template is apparent. The dashed line indicates the demarcation between polymer-filled and empty pSi regions. Scale bar: 2 μm. (c) Higher magnification cross-sectional image of the empty region of the pSi film (above the dashed line in (b)), representing ~6 cycles of the repeating rugate nanostructure in the porous film. Scale bar: 200 nm. At this magnification, the gradual oscillations in porosity that occurs in the nanostructure to generate the optical rugate filter are not readily apparent. (d) Cross-sectional image obtained at the same magnification as in (c), but of the polycarbonate-filled region of the pSi film (below the dashed line in (b)). Scale bar: 200 nm. (e) EDS element map of approximately the same region as represented in (b), showing the boundary and depth of polymer infiltration (green represents silicon and red represents carbon). Scale bar: 2.5 μm. (f) Cross-sectional image of the all-polymer photonic sensor for comparison. This sample was prepared by thermal infiltration of a pSi template with polycarbonate as in the other images, but the silicon nanostructure has been removed by selective dissolution using dimethyl sulfoxide/HF(aq) as described in the text. Scale bar: 1 μm.

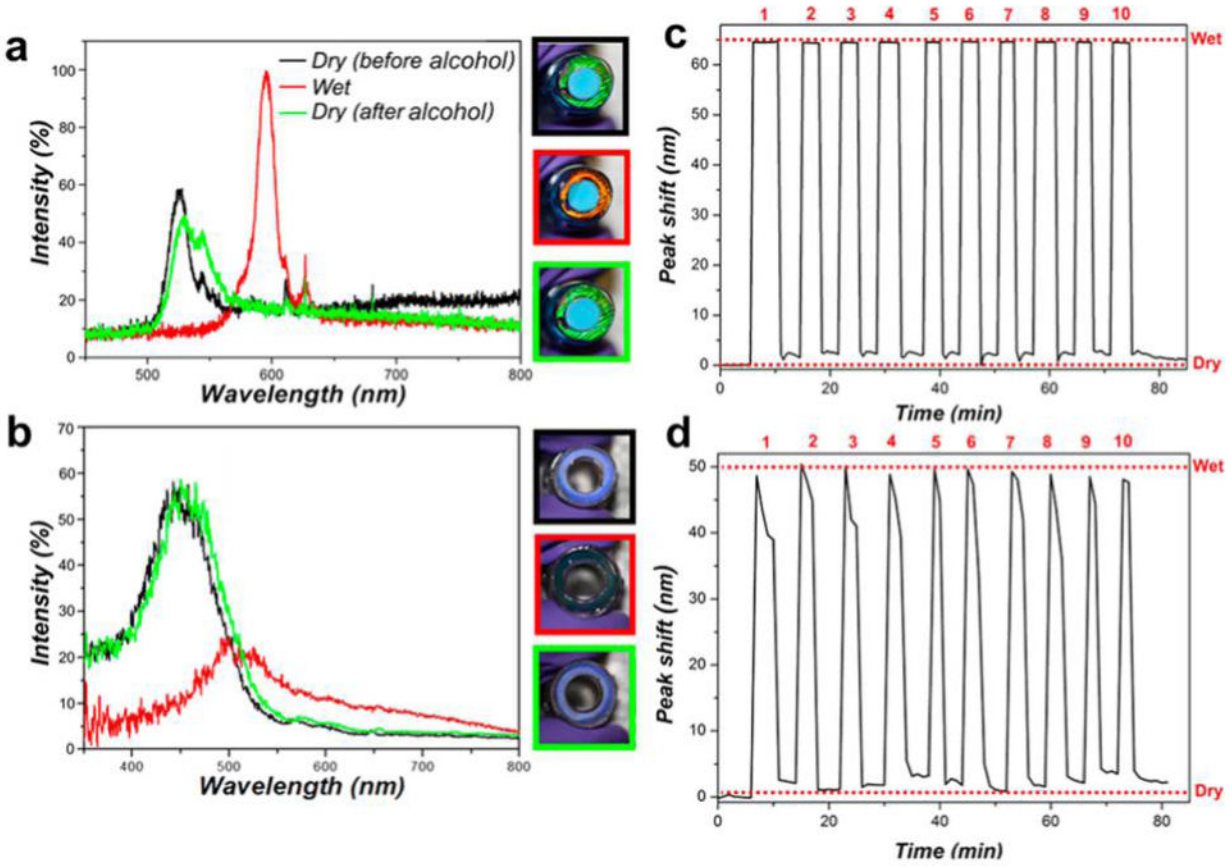

Figure 2.

Spectral shifts and reproducibility of pSi-polymer composite and all-polymer photonic sensors embedded in IV connector hub units. Reflected light spectra quantify the shift in the photonic stop-band when 70% isopropyl alcohol sterilization solution is applied: (a) pSi-polymer composite photonic sensor; (b) all-polymer photonic sensor. Images at the right of each plot show digital photographs of the IV connector hub units corresponding to the traces: top, dry sensor prior to alcohol; middle, sensor wetted with alcohol; bottom, sensor after a few minutes of air-drying. Border color of each photograph corresponds to the color of each representative trace in the plots. (c,d) Changes in the wavelength of the reflection stop-band, recorded during repeated exposure of (c) composite IV connector hub unit and (d) all-polymer IV connector hub unit to 70% isopropyl alcohol solution. Peak shift values correspond to the increase in wavelength (red shift) of the stop band when the porous nanostructure is fully wetted with 70% isopropyl alcohol solution (“Wet”) relative to the dry, air-filled sensor (“Dry”). The number of sterilization cycles is indicated on the top.

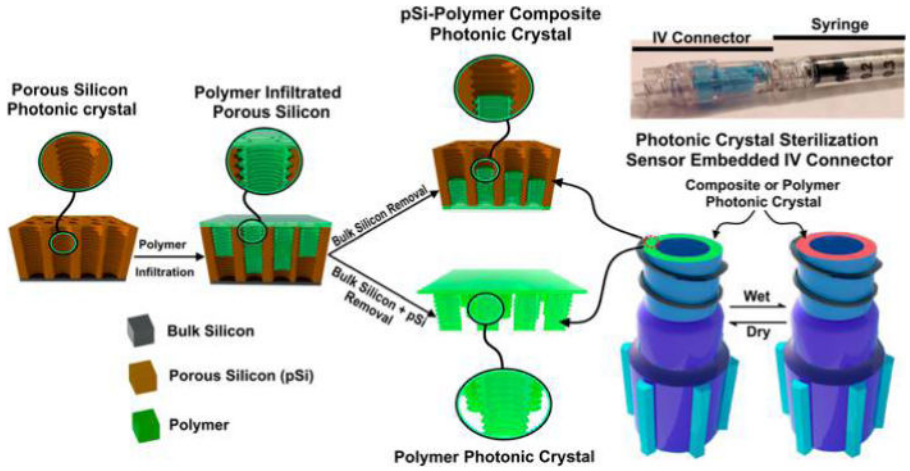

Scheme 1. Schematic of the Steps Used to Prepare pSi–polymer Composites and All-Polymer Photonic Crystals Used as Sterilization Sensors[a]

[a]First, a pSi template is prepared by electrochemical etching using a sinusoidal current density-time waveform, such that it possesses a layered porous nanostructure that acts as a 1-dimensional photonic crystal. Then the polymer (in this work, a test article or a commercial IV connector hub) is thermally infiltrated into the pores of the pSi template by raising its temperature above the glass transition temperature of the polymer (230 °C for the polycarbonate used in this work). To prepare the pSi-polymer composite photonic crystal, the polymer is only partially infiltrated into the pSi nanostructure, and the thermally infiltrated structure separates from the silicon wafer substrate upon cooling. For the all-polymer photonic crystal, the composite is removed by freeze-fracture, and then the nanostructured pSi template is removed by chemical dissolution using a mixture of dimethyl sulfoxide, aqueous HF, and ethanol. A photograph of a sensor-embedded IV connector hub mated to a syringe is shown on the upper right. The tip of the hub where the photonic sensor is located attaches to the syringe through a luer lock fitting, and the opposite end of the hub connects to an IV line. Under normal operation, the luer lock isolates the sensor element from the fluid being delivered and there is no contact between the IV fluid and the sensor.